https://doi.org/10.2352/ISSN.2470-1173.2018.13.IPAS-219

Color Visibility Images and Measures of Image Enhancement

Artyom Grigoryan and Sos Agaian*, Department of Electrical and Computer Engineering, The University of Texas at San Antonio, USA, *Computer Science Department, College of Staten Island and the Graduate Center, Staten Island, NY, USA

Abstract

In this paper, we introduce the human visual system-based several new (a) methods to visualize the very small differences in intensities without big changes of primary image information and (b) measures that quality the visuality of both grayscale and color images. Several illustrative examples are also presented. The proposed concepts can be used for many image processing, computer vision and recognition system applications.

Introduction

Edges and contrast (the separation between the darkest and brightest local areas of the image) of view are the most important characteristics of detail discrimination of an image. As well, the information of edges in objects can be extracted by gradient operators that calculate the local difference in each pixel with its neighbors [1]-[3],[14,15]. The human visual systems have difficulties to distinct image details and edges when a small number of gray values brighter than their background. This problem is very crucial for image processing, computer vision and recognition system applications, for instance face, object and action recognition systems, microscopic (fluorescence) image analysis, or, interpretation /understanding of images. Therefore, it is important to have a tool that a) visualizes the very small differences in intensities without big changes of primary image information; b) can distinguish a wide range of color hues; c) measures the quality of visuality of both grayscale and color images; and d) quantifies the intensity relationship changes within an image.

The goal of this paper is to improve the visibility (detail discrimination of an image) of gray, color and video sequences in different scales, including the logarithmic scale. We introduce the human visual system based several new gradient operators for color images. The concepts of Weber-Fisher law-related visibility operators and images are presented as important characteristics of the image that can be used for instance in object and face recognition. We also consider the visibility images related to the Michelson contrast and EME type measures as tools in face detection, and facial image representation. To measure the quality of images and select optimal processing parameters, the EME measure was successfully used for image enhancement of grayscale images [4]-[7] and color images transformed to quaternion space [29]-[34]. This measure can be compared with the Weber-Fechner law of the human visual system. Weber stated that the smallest noticeable change in the image intensity is proportional to the original intensity (before adding the difference). As an example, Fig. 1 shows the color "peppers" image in part (a). The color image composed by the measure EME visibility color images (EVI) of three color components of the image is shown in part (b) and the grayscale component of the color EVI in part (c).

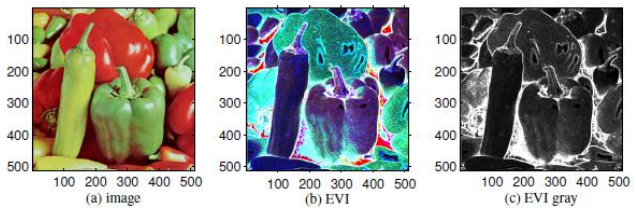

***Figure 1**. (a) The color image, (b) the EVCI, and (c) the grayscale image of the EVCI.*

The Weber visibility images can be processed in different scales, by using the known monotonic functions, including the logarithm, arctangent, square root, and the 3rt root. The sine function also can be used, since the values of the ratio are considered to vary from the small number 1/255 to maximum 1 in the absolute scale. All presenting concepts of visibility images can be applied component-wise for color images in the RGB and other color models. Examples of visibility color images are given.

Quantitative Enhancement Measure

To measure the quality of images and select optimal processing parameters, we consider the described in [4,5] quantitative measure of image enhancement that is based on the ratio of the maximum and minimum of intensity in the logarithm scale. The image enhancement measure estimation (EME) is based on the idea of calculating a visibility image which is defined as the ratio of maximums and minimums. This image enhancement measure can be used for selecting the best parameters for image enhancement by the Fourier transform, as well as other unitary transforms [6]. The visibility images are related to measures of image enhancement that are used to estimate quantitatively a quality of the image after enhancement in grays or colors [20,34]. The measure is defined as follows (a review of the quantitative enhancement measure can be found in Refs. [8]-[13] and [16]-[28]). The image $f_{n,m}$ of size $N \times M$ is divided by small blocks of size 7×7 each, for instance, with number along the dimensions $k_1 = \lfloor N/7 \rfloor$ and $k_2 = \lfloor M/7 \rfloor$ with the floor rounding. Blocks of sizes 5×5, 6×6, 8×8, and 9×9 can also be used is such a division of image. The measure of the image after enhancement, $f_{n,m} \to g_{n,m}$, is defined by

$$EME(g) = \frac{1}{k_1 k_2} \sum_{k=1}^{k_1} \sum_{l=1}^{k_2} 20 \ln \frac{\max_{k,l}(g)}{\min_{k,l}(g)}. \qquad (1)$$

Here, $\max_{k,l}(g)$ and $\max_{k,l}(g)$ respectively are the maximum and minimum of the image $g_{n,m}$ inside the (k,l)th block. $EME(g)$ is called a measure of enhancement, or measure of improvement of the image f. The max/min ratios in Eq. 1 can be written as

$$EME(g) = \frac{1}{k_1 k_2} \sum_{k=1}^{k_1} \sum_{l=1}^{k_2} 20 \left[\ln \max_{k,l}(g) - \ln \max_{k,l}(g) \right].$$

It shows the range of intensity of the image in the logarithm scale. The measure $EME(g)$ determines the average-block scale of intensity in the image. If the image enhancement is parameterized by a parameter α, i.e., the image $g = g_\alpha$, then we can define the best or optimal parameter α_0, such that the EME has a maximum at this point. The value of $EME(f)$ is called the enhancement measure of the original image f.

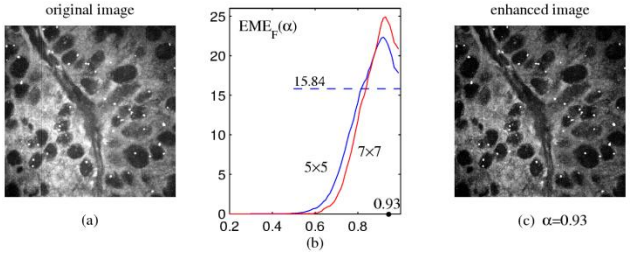

***Figure 2.** (a) The original grayscale image, (b) two graphs of the EME measure, $EME(\alpha)$, and (c) the image enhanced by parameter α_0 =0.93.*

As an example, Fig. 2 shows the image in part (a), that is enhanced by the a-rooting method, when the magnitude of the 2-D DFT of the image $F_{p,s}$ is changed by $|F_{p,s}| \to |F_{p,s}|^{\alpha}$ [5]-[7]. For the original image, $EME(f) = 15.84$. Two graphs of the EME measure that are calculated by using 5×5 and 7×7 blocks are given in part (b). The parameter a varies in the interval [0.35,1]. The curves have pikes of maximum at the same point 0.93. The 0.93-rooting enhancement of the image is shown in part (c). The enhancement equals $EME(g) = 25.03$.

Weber-Fechner Visibility Images

We consider measures that are related to the Weber-Fechner law of the human visual system. It was stated that in the image intensity, the smallest noticeable change, Δf, is proportional to the original intensity f,

$$|\Delta f|/f \approx \text{const} \approx 0.015.$$

According to Fechner, this ratio should be considered as

$$k\frac{|\Delta f|}{f + f_0} \approx \text{const},$$

where k is constant and f_0 is the smallest value of intensity [33]. The value 0.015 was estimated experimentally and it called the Weber fraction. The difference operator Δf at the pixel (n, m) can be written as

$$(\Delta f)_{n,m} = f_{n,m} - \text{Mean}(f_{n,m}),$$

where the mean operator can be calculated by windowed convolution with masks of size 3×3 or 5×5. For instance, the cross and square masks can be used. The first order Weber visibility image is defined as

$$W(f)_{n,m} = k\frac{\left|f_{n,m} - \alpha\text{Mean}(f_{n,m})\right|}{f_0 + f_{n,m}}, \qquad (2)$$

where k and $\alpha > 0$ are constants [33].

As an example, Figure 3 shows the "pepper" image in part (a) and the Weber visibility image in part (b), which is calculated by using the 3×3 cross-window.

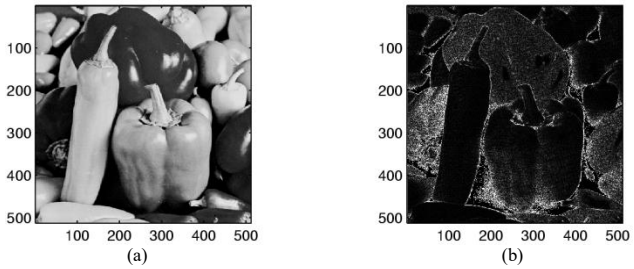

Figure 3. *(a) The grayscale image. (b) The Weber visibility image.*

In the definition of visibility image, the 2nd order gradients can also be used. The visibility image is considered as an important characteristic that describes small noticeable changes in the intensity of the image.

We also consider the "cameraman" image that is shown in Fig. 4 in part (a). The Weber visibility image of this image is shown in part (b); this image is calculated by using the 3×3 cross window.

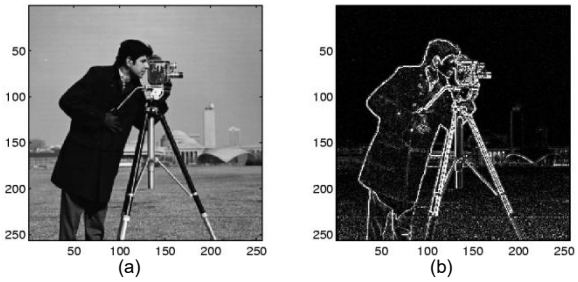

Figure 4. *(a) The "cameraman" image. (b) The Weber visibility image.*

Different scales can be used when calculating the Weber visibility images, and for that many known monotonic functions can be used, including the logarithm, arctangent, square root, and the 3rt root. The Weber visibility image $W(n, m)$ can also be modified by using the sine function with a given frequency ω_0 as proposed by Grigoryan [33],

$$A: f_{n,m} \to A(f)_{n,m} = \sin\left[\omega_0 A(f)_{n,m}\right].$$

Figure 5 shows such visibility images for the "cameraman" image, which are calculated with $\omega_0 = 0.75,\ 0.5$, and 0.35 in parts (a), (b), and (c), respectively.

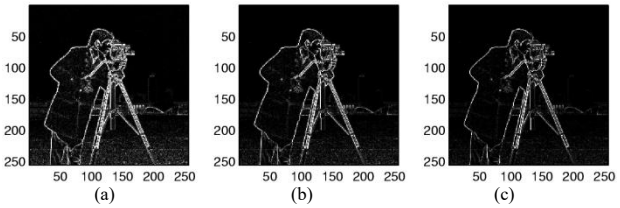

Figure 5. *The Weber-Grigoryan visibility image for the frequency ω_0 equal (a)* 0.75 *(b)* 0.5 *and (c)* 0.35.

Michelson Visibility Images

The visibility images with Michelson contrast definition are calculated by using the ratios of difference of the local maximum and minimum to their sum at each pixel. The visibility image is defined as [27]

$$C(f)_{n,m} = k\frac{\max_W(f_{n,m}) - \min_W(f_{n,m})}{\max_W(f_{n,m}) + \min_W(f_{n,m})}, \qquad (3)$$

where k is a constant. The image $C(f)_{n,m}$ is called t*he Michelson visibility image* of the image $f_{n,m}$.

For the "peppers" image, Fig. 6 shows the Michelson visibility image for in part (a) and the Weber visibility image in part (b), for comparison.

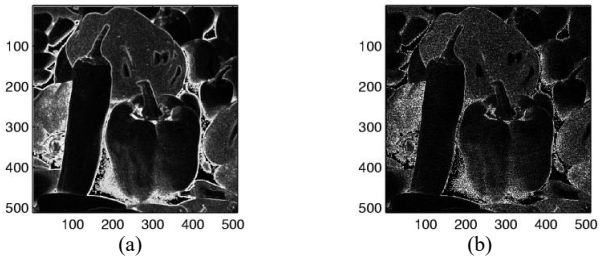

Figure 6. *(a) The Michelson visibility "cameraman" image. (b) The Weber visibility image.*

Different modifications of the Michelson visibility image can be used, including the following Agaian-DelMarco visibility images:

$$C_4(f)_{n,m} = k\frac{\sqrt{[\max_W(f_{n,m}) - f_{n,m}][f_{n,m} - \min_W(f_{n,m})]}}{\max_W(f_{n,m}) + \min_W(f_{n,m})}$$

and

$$C_5(f)_{n,m} = k\sqrt{\frac{[\max_W(f_{n,m}) - f_{n,m}][f_{n,m} - \min_W(f_{n,m})]}{[\max_W(f_{n,m}) + f_{n,m}][f_{n,m} + \min_W(f_{n,m})]}}.$$

As an example, for the "pepper" image, Fig. 7 shows the 4th Michelson visibility image $C_4(f)_{n,m}$ in part (a), and the 5th Michelson visibility image $C_5(f)_{n,m}$ in part (b).

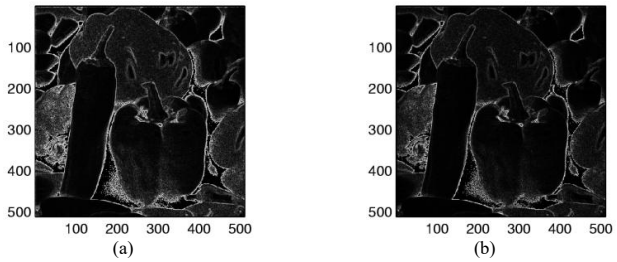

Figure 7. *The Michelson visibility "cameraman" image (a) $C_4(f)$ and (b) $C_5(f)$.*

Visibility Measures Related to EMEs

The enhancement measure EME calculates the average range of intensity of the image in the logarithm scale and the enhancement of the image $f_{n,m}$ is the estimated block-wise. In the general case, instead of square blocks, we can consider the maximum and minimum operations as local operations with the chosen small window W. These operations we denote by $\max_W$ and $\min_W$, respectively. Then, the EME related visibility image at the pixel (n,m) can be defined as follows:

$$E(f)_{n,m} = \text{kln}\left[\frac{\max_W(f_{n,m})}{\min_W(f_{n,m})}\right], \quad (4)$$

where k is a constant. If $\min_W(f_{n,m}) = 0$, the value $E(f)_{n,m}$ is considered to be zero. Also, we can add a small number $\varepsilon_0 > 0$ in the denominator in this ratio. The image $E(f)_{n,m}$ is called *the EME visibility image* of $f_{n,m}$.

As an example, Fig. 8 shows the EME visibility "peppers" image in part (a), which was calculated for the square 3×3-window. The same image in the logarithm scale is shown in part (b), and the Michelson visibility image is given in part (c), for comparison.

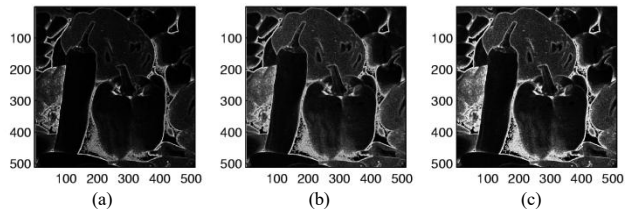

Figure 8. *(a) The EME measure visibility image. (b) The image in (a) in the logarithm scale. (c) The Michelson visibility image.*

It is interesting to note that the EME visibility image can also be defined by using the same definition on the EME visibility image itself, instead of the original image. In other words, the following image is calculated

$$LE(f)_{n,m} = \text{kln}\left[\frac{\max_W\left(E(f_{n,m})\right)}{\min_W\left(E(f_{n,m})\right)}\right]. \quad (5)$$

It is clear that the EME measure can be calculated from its EME visibility image as the sum of values of the visibility image at centers of blocks. If the size of blocks is 3×3, the EME image calculated only at the centers of the blocks is a down-sampled representation of the EME image.

Color Visibility Images

The concepts of visibility images can be applied component-wise for color images. In the known RGB color model [1], the color image is represented at each pixel as $f_{n,m} = (r_{n,m}, g_{n,m}, b_{n,m})$. The EME visibility color image (EVCI) is defined by

$$E(f_{n,m}) = [E(r_{n,m}), E(g_{n,m}), E(b_{n,m})],$$

where the color components of this image are calculated as

$$E(r_{n,m}) = \text{kln}\left[\frac{\max_W(r_{n,m})}{\min_W(r_{n,m})}\right],$$
$$E(g_{n,m}) = \text{kln}\left[\frac{\max_W(g_{n,m})}{\min_W(g_{n,m})}\right],$$
$$E(b_{n,m}) = \text{kln}\left[\frac{\max_W(b_{n,m})}{\min_W(b_{n,m})}\right].$$

As an example, Fig. 1 shows the color "peppers" image in part (a). The color image composed by the measure EME visibility images (EVI) of three color components of the image is shown in part (b) and the grayscale component of the EVCI in part (c).

The color components of the multiplicative visibility color image (MEVCI) are calculated by

$$E(c_{n,m}) = \text{kln}\left[\frac{\max_W(c_{n,m})}{\min_W(c_{n,m})}\right](c_{n,m})^{\beta}, \quad (6)$$

where β is the new parameter. The image $c_{n,m}$ is one of the color image components. For the case when β=1, Fig. 9 shows the MEVCI of the "peppers" image in part (a) and its grayscale component in (b).

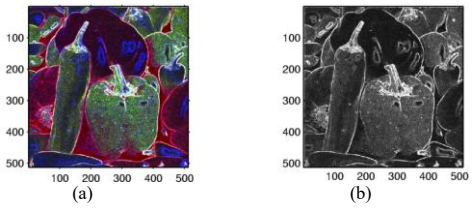

Figure 9. *(a) The MEVCI of the "peppers" image and (b) the grayscale image of the MEVCI.*

We also consider the β=1 case with the color "flowers" image that is shown in Fig. 10 in part (a). The color image composed by the EME visibility images of three color components is shown in part (b) and the grayscale component of this image in part (c).

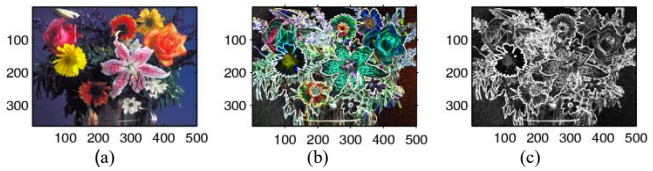

Figure 10. *(a) The color "flowers" image, (b) the MEVCI, and (c) grayscale image of the MEVCI.*

Figure 11 shows the multiplicative MEVCI of the "flowers" image. The color image is in part (a) and its grayscale image in part (b).

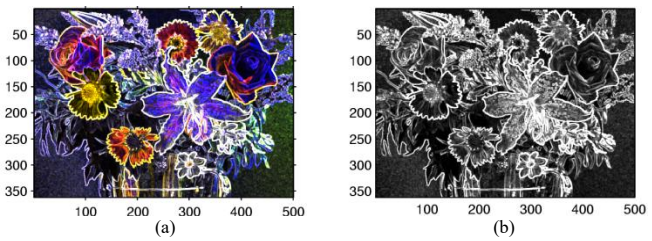

Figure 11. *(a) The color "flowers" MEVCI image, and (c) the grayscale image of the MEVCI.*

Other Multiplicative Visibility Color Images

The Weber visibility color image (WVCI) is defined by the operator

$$V(f_{n,m}) = [V(r_{n,m}), V(g_{n,m}), V(b_{n,m})]$$

where the color components of this image are calculated as

$$V(c_{n,m}) = \mathrm{k}\frac{|c_{n,m} - \max_W(c_{n,m})|}{c_{n,m} + \varepsilon_0}, \quad (7)$$

Here, the image $c_{n,m}$ is used for color components $r_{n,m}$, $g_{n,m}$, and $b_{n,m}$.

As an example, Fig. 12 shows the color "peppers" image in part (a), and the color image composed by the Weber visibility images of three color components, the red, green, and the blue, in part (b). The grayscale component of the visibility image is shown in part (c).

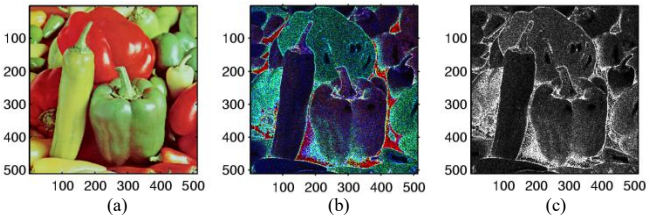

Figure 12*. (a) Color image, (b) the WVCI image, and (c) the grayscale image of the WVCI.)*

The Michelson visibility color image (MVCI) is defined by the operator

$$C(f_{n,m}) = [C(r_{n,m}), C(g_{n,m}), C(b_{n,m})],$$

where the color components of this image are calculated by

$$C(c_{n,m}) = \mathrm{k}\frac{|\max_W(c_{n,m}) - \min_W(c_{n,m})|}{\max_W(c_{n,m}) + \min_W(c_{n,m})}. \quad (8)$$

The multiplicative Michelson visibility color image is defined with the color components that are calculated by

$$C(c_{n,m}) = \mathrm{k}\left[\frac{|\max_W(c_{n,m}) - \min_W(c_{n,m})|}{\max_W(c_{n,m}) + \min_W(c_{n,m})}\right](c_{n,m})^{\beta}. \quad (9)$$

As an example, Fig. 13 shows the color "peppers" image in part (a), and the color image composed by the Michelson visibility images (MVI) of three color components in part (b). The grayscale component of the MVCI is shown in part (c).

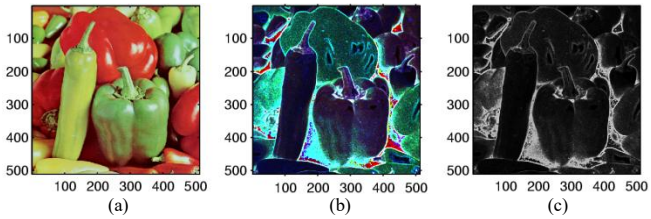

Figure 13. *(a) Color image, (b) the MVCI image, and (c) the grayscale image of the MVCI.*

Summary

The concepts of the color visibility images have been introduced with examples that include the related to the Weber-Fisher visual law and Michelson contrast definition, as well as new visibility images that can be used in color image representation and processing, computer vision and recognition system applications.

References

[1] R.C. Gonzalez, R.E. Woods, Digital Image Processing, 2nd Edition, Prentice Hall, Upper Saddle River, New Jersey, 2002.

[2] B.K.P. Horn, Robot Vision, The MIT Press, Cambridge, 1986.

[3] W.K. Pratt, Digital Image Processing, 3rd Edition, John Wiley & Sons, Inc., 2001.

[4] S.S. Agaian, K. Panetta, A.M. Grigoryan, "A new measure of image enhancement," Proc. IASTED Int. Conf. Signal Processing &Communication, Marbella, Spain, 19–22 (2000).

[5] S.S. Agaian, K. Panetta, A.M. Grigoryan, "Transform-based image enhancement algorithms," IEEE Trans. on Image Processing, vol. 10, no. 3, pp. 367–382, 2001.

[6] A.M. Grigoryan, S.S. Agaian, Multidimensional Discrete Unitary Transforms: Representation, Partitioning and Algorithms, Marcel Dekker Inc., New York, 2003.

[7] A.M. Grigoryan, S.S. Agaian, "Transform-based image enhancement algorithms with performance measure," Advances in Imaging and Electron Physics, Academic Press, vol. 130, pp. 165–242, 2004.

[8] A.M. Grigoryan and S.S. Agaian, "Adapted Retinex Algorithm with Complexity Optimization for Mobile Phone Medical Image Enhancement," - chapter 5, pp. 119-151. In Electronic Imaging Applications in Mobile Healthcare, J. Tang, S.S. Agaian, and J. Tan, Eds., SPIE Press, Bellingham, Washington, February 2016,

[9] F.T. Arslan, A.M. Grigoryan, "Fast splitting alpha-rooting method of image enhancement: Tensor representation," IEEE Trans. on Image Processing, vol. 15, no. 11, pp. 3375–3384, Nov. 2006.

[10] A.M. Grigoryan, S.S. Agaian, "Monotonic sequences for image enhancement and segmentation," Digital Signal Processing, vol. 41, pp. 70–89, June 2015, (doi:10.1016/j.dsp.2015.02.011)

[11] A.M. Grigoryan, S.S. Agaian, "Preprocessing Tools for Computer-Aided Cancer Imaging Systems," in "Computer-Aided Cancer Detection and Diagnosis: Recent Advances" (Editors: J. Tang and S. Agaian), SPIE, chapter 2, p. 55, 2014.

[12] A.M. Grigoryan, M. Hajinoroozi, "Image and audio signal filtration with discrete Heap transforms," Applied Mathematics and Sciences: An International Journal (MathSJ), vol. 1, no. 1, pp. 1-18, May 2014.

[13] A.M. Grigoryan, M.M. Grigoryan, Brief Notes in Advanced DSP: Fourier Analysis With MATLAB, CRC Press, Taylor and Francis Group, Boca Raton, New York, 2009.

[14] D. Marr, E. Hildrith, "Theory of edge detection," Proc. Royal Society of London, vol. B207, pp. 187-217, 1980.

[15] P. Zamperoni, "Image enhancement," Advanced in Image and Electron Physics, vol. 92, pp. 1–77, 1995.

[16] E.A. Silva, K.A. Panetta, S.S. Agaian, "Quantify similarity with measurement of enhancement by entropy," Proc. SPIE, vol. 6579, 65790U, 2007.

[17] K.A Panetta, E.J. Wharton, S.S. Agaian, "Human visual system-based image enhancement and logarithmic contrast measure, " IEEE Transactions on Systems, Man, and Cybernetics, Part B (Cybernetics), vol. 38, no. 1, pp. 174–188, 2008.

[18] E. Wharton, S. Agaian, K. Panetta, "A logarithmic measure of image enhancement," Proc. SPIE, vol. 6250, 62500P, 2006.

[19] E. Wharton, K Panetta, S. Agaian, "Human visual system based similarity," Proc. Systems, Man and Cybernetics,. SMC 2008. IEEE International Conference on, pp. 685–690, 2008.

[20] S. Agaian, "Visual morphology," Proc. SPIE, 3646, 1999.

[21] K.A. Panetta, C. Gao, S.S. Agaian, "No reference color image contrast and quality measures, " IEEE Transactions on Consumer Electronics, vol. 59, no. 3, pp. 643–651, 2013.

[22] A.M. Grigoryan, S.S. Agaian, "Color Enhancement and Correction for Camera Cell Phone Medical Images Using Quaternion Tools," Chapter 4, pp. 77–117. In book: Electronic Imaging Applications in Mobile Healthcare, (J. Tang, S.S. Agaian, and J. Tan, Eds.,) SPIE Press, Bellingham, Washington, 2016.

[23] S.C. Nercessian, S.S. Agaian, K.A. Panetta, "Multi-scale image enhancement using a second derivative-like measure of contrast," Proc. SPIE, vol. 8295, 82950Q, 2012.

[24] R. Kogan, S. Agaian, K.A. Panetta, "Visualization Using Rational Morphology and Zonal Magnitude Reduction," Proc. SPIE, vol. 3304, 1998.

[25] E. Wharton, S. Agaian, K. Panetta, "Adaptive Multi-Histogram Equalization using Human Vision Thresholding," SPIE Electronic Imaging, 2007.

[26] K. Panetta, L. Bao, S. Agaian, "A human visual "no-reference image quality measure," IEEE Instrumentation & Measurement Magazine, vol. 19, no. 3, pp. 34–38, 2016.

[27] C. Gao, K. Panetta, S. Agaian, "Color image attribute and quality measurements," Proc. SPIE, vol. 9120, 91200T, 2014.

[28] C. Gao, K. Panetta, S. Agaian, "No reference color image quality measures," Cybernetics (CYBCONF), 2013 IEEE International Conference on, pp. 243–248, 2013.

[29] A.M. Grigoryan, J. Jenkinson, S.S. Agaian, "Quaternion Fourier transform based alpha-rooting method for color image measurement and enhancement," SIGPRO-D-14-01083R1, Signal Processing, vol. 109, pp. 269–289, April 2015, (doi:10.1016/j.sigpro.2014.11.019)

[30] A.M. Grigoryan, S.S. Agaian, "Retooling of color imaging in the quaternion algebra," Applied Mathematics and Sciences: An International Journal (MathSJ), vol. 1, no. 3, pp. 23–39, 2014.

[31] A.M. Grigoryan, S.S. Agaian, "Alpha-rooting method of color image enhancement by discrete quaternion Fourier transform," Proc. SPIE, vol. 9019, 901904, 2014.

[32] A.M. Grigoryan, J. Jenkinson, S.S. Agaian, "Quaternion Fourier transform based alpha-rooting method for color image measurement and enhancement," SIGPRO-D-14-01083R1, Signal Processing, vol. 109, pp. 269–289, 2015.

[33] A.M. Grigoryan, S.S. Agaian, Practical Quaternion Imaging With MATLAB, SPIE PRESS, 2018.

[34] A.M. Grigoryan, S.S. Agaian, "Image Processing Contrast Enhancement," 22p, Wiley Encyclopedia of Electrical and Electronics Engineering, May 2017 (doi: 10.1002/047134608X.W5525.pub2)

Author Biography

Artyom Grigoryan received the MS degrees in mathematics from Yerevan State University (1978), in imaging science from Moscow Institute of Physics and Technology (1980), and in electrical engineering from Texas A&M University (1999), and PhD degree in mathematics and physics from Yerevan State University (1990). He is an associate professor of the ECE Department, College of Engineering, University of Texas at San Antonio. He is author of 4 books, 10 book-chapters, 3 patents, 120 papers.

Sos Agaian received the M.S. degree in mathematics and mechanics from Yerevan University, Armenia, the Ph.D. degrees in math and physics from Steklov Institute of Mathematics, Russian Academy of Sciences, and in engineering from Institute of Control System, Russian Academy of Sciences. He is professor of the Science Department, College of Staten Island. He is Fellow of the SPIE, IEEE, AAAS, and IS&T. He has authored of 500 scientific papers, 7 books, holds 14 patents.